

Fluctuations of Permeable Interfaces in Water-in-Water Emulsions

Leonard M. C. Sagis

Physics Group, Department ATV, Wageningen University, Bomenweg 2, 6703 HD Wageningen, The Netherlands
(Received 13 September 2006; published 9 February 2007)

The fluctuations of highly permeable interfaces, encountered in phase-separated biopolymer solutions, liposomes, polymersomes, or colloidosomes, are investigated. An expression for the power spectrum of the height correlation function is derived for a multicomponent system, incorporating the effects of mass transfer across the interface, using nonequilibrium thermodynamics. We also derive an expression for the relaxation time of the height correlation function, and calculate the relaxation time for a phase-separated gelatin-dextran-water system. Comparing our expression with the expression for an impermeable interface shows that mass transfer has a significant impact on the relaxation time of the interface.

DOI: [10.1103/PhysRevLett.98.066105](https://doi.org/10.1103/PhysRevLett.98.066105)

PACS numbers: 68.35.Ja, 68.05.-n

Water-in-water emulsions, such as phase-separated (bi-)polymer solutions, liposomes, polymersomes, or colloidosomes, can be used for encapsulation and texturing applications in pharmaceutical, food, or cosmetic products. The interfaces in these emulsions have properties that differ significantly from those found in oil-water or water-air systems, stabilized by a simple surfactant. The interfacial tension in water-in-water emulsions is often extremely low. For example, in phase-separated biopolymer solutions the surface tension is of the order of 10^{-6} N/m [1]. The bending rigidity of interfaces in these systems can be significant, as high as 500 kT [2]. As a result, the bending rigidity can have an appreciable effect on the dynamic behavior of these systems [3].

Another important property of the interfaces in water-in-water emulsions is their permeability. In these systems water and dissolved molecules can transfer easily from one aqueous bulk phase to the other. This high permeability of the interface has a significant effect on the stress-deformation and deformation-relaxation behavior of, for example, droplets in phase-separated biopolymer solutions [4,5].

That mass transfer can have an appreciable effect on the dynamic behavior of a deformed droplet was also shown in recent interfacial tension measurements of biopolymer solutions, using the spinning drop method [6]. Droplets deformed by spinning the capillary, slowly dissolved, and the rate of dissolution increased with increasing spinning rate, or increasing deformation of the droplets.

In previous work we used scaling analysis to study the effects of permeability and bending rigidity on the dynamic behavior of phase-separated biopolymer solutions [4–6]. In systems with a composition close to the critical point, we observed that the relaxation time of the system scales as $\tau \sim L^4/(\lambda_p k)$, with L a characteristic length scale of the system, λ_p the permeability of the interface, and k the bending rigidity. In systems with a composition far from the critical point, relaxation is dominated by surface tension γ and permeability, and $\tau \sim L^2/(\gamma \lambda_p)$.

Here we will use a more formal approach, using nonequilibrium thermodynamics to derive expressions for the power spectrum of the height correlation function and the relaxation time of the interface, which incorporate the effects of mass transfer. The model presented here is an extension of the development by Flekkøy and Rothman [7], for the thermal fluctuations of interfaces between simple fluids. We will illustrate the effects of permeability and bending rigidity on the dynamics of these systems by calculating the relaxation time for a phase-separated gelatin-dextran-water system. This relaxation time is an important parameter, since it also describes the relaxation of small mechanical perturbations of the interface during production, processing and application of these systems. The calculations of the relaxation time confirm the scaling regimes found earlier in [5]. Although the primary focus of this Letter will be on phase-separated biopolymer solutions, the results of this analysis are also applicable to phase-separated aqueous polymer-colloid systems, liposomes, polymersomes, or colloidosomes.

We will make the following assumptions in analyzing this problem: (i) For the sake of simplicity, we will neglect any effects from the macroscopic curvature of the droplets, and assume the equilibrium interface is a horizontal flat interface located at $z = 0$, separating two liquid bulk phases. This assumption is valid as long as the perturbations of the interface are small compared to the radius of the droplet. The equilibrium state of the system is given by $\mathbf{v}^{(i)} = \mathbf{0}$, $\rho^{(i)} = \bar{\rho}^{(i)}$, $\rho_{(A)}^{(i)} = \bar{\rho}_{(A)}^{(i)}$, and $P^{(i)} = \bar{P}^{(i)}(z)$. Here, $\mathbf{v}^{(i)}$ is the velocity in bulk phase i ($i = 1, 2$), $\rho^{(i)}$ the total density in phase i , $\rho_{(A)}^{(i)}$ the mass density of species A in phase i , and $P^{(i)}$ the pressure. A bar “—” will be used to denote equilibrium values of a variable. The system is a multicomponent system with N components. (ii) We will limit ourselves to perturbations in the xz plane. In a Cartesian coordinate system the parametrization of the perturbed interface is given by $z = h(x, t)$, and the perturbed state of the system is given by

$$\begin{aligned} \mathbf{v}_x^{(i)} &= \mathbf{v}_x^{(i)}(x, z), & \mathbf{v}_y^{(i)} &= 0, & \mathbf{v}_z^{(i)} &= \mathbf{v}_z^{(i)}(x, z), \\ \rho_{(A)}^{(i)} &= \bar{\rho}_{(A)}^{(i)} + \delta\rho_{(A)}^{(i)}(x, z), & \rho^{(i)} &= \bar{\rho}^{(i)} + \delta\rho^{(i)}(x, z), \\ P^{(i)} &= \bar{P}^{(i)}(z) + \delta P^{(i)}(x, z). \end{aligned} \quad (1)$$

(iii) The dividing surface is only weakly deformed, in the sense that $[\partial h(x, t)/\partial x]^2 \ll 1$. This implies that the non-zero components of the unit normal vector of the interface $\boldsymbol{\xi}$, and the curvature of the interface are given by

$$\xi_x = -\left(\frac{\partial h(x, t)}{\partial x}\right), \quad \xi_z = 1, \quad H = \frac{1}{2} \frac{\partial^2 h(x, t)}{\partial x^2}. \quad (2)$$

(iv) The fluid phases on both sides of the interface are assumed to be Newtonian, with constant shear viscosity $\eta^{(i)}$, and constant bulk viscosity $\eta_b^{(i)}$. We will also assume that inertial effects can be neglected in the momentum balances. No body forces are acting on the material in the bulk phases. (v) The dividing surface between the two bulk phases is located such that the surface mass density is negligible ($\rho^s \approx 0$). We will neglect any contributions from surface viscosities and surface elasticities to the surface stress tensor [8]. This is a valid assumption for phase-separated biopolymer solutions, but for polymerosomes or colloidosomes these contributions may be important, especially when deformations of the interface are large. We will discuss how to account for these effects at the end of this Letter. For the surface tension γ we will use the Helfrich expansion [9], assuming zero spontaneous curvature and neglecting contributions from the Gaussian curvature:

$$\gamma = \gamma_0 + kH^2. \quad (3)$$

The surface tension of the flat interface γ_0 and the bending rigidity k are assumed to be constant. The capillary numbers satisfy $N_{Ca}^{(i)} \ll 1$, and inertial effects will be neglected in the jump momentum balance [8]. (vi) The system is isothermal, and we will neglect all contributions from heat transfer in the differential energy balance.

With assumption (ii) the linearized equation of continuity reduces to

$$\frac{\partial \delta \rho^{(i)}}{\partial t} + \bar{\rho}^{(i)} \text{div} \mathbf{v}^{(i)} = 0. \quad (4)$$

Since we allow for mass transfer across the interface, the densities on both sides of the interface change in time, and we cannot set the first term in (4) to zero. In view of assumption (ii) and (iv), the differential momentum balance for each bulk phase reduces to

$$\nabla P^{(i)} = \text{div} \boldsymbol{\sigma}^{(i)} + \mathbf{f}^{h(i)}, \quad (5)$$

where $\boldsymbol{\sigma}^{(i)} = \nu^{(i)}(\text{div} \mathbf{v}^{(i)})\boldsymbol{\delta} + 2\eta^{(i)}\mathbf{D}^{(i)}$ is the extra stress tensor, $\nu^{(i)} = \eta_b^{(i)} - \frac{2}{3}\eta^{(i)}$, $\boldsymbol{\delta}$ the unit tensor, $\mathbf{D}^{(i)}$ the rate of deformation tensor, and $\mathbf{f}^{h(i)}$ the force resulting from thermal fluctuations. The linearized differential mass bal-

ance for species A is given by

$$\frac{\partial \delta \rho_{(A)}^{(i)}}{\partial t} + \bar{\rho}_{(A)}^{(i)} \text{div} \mathbf{v}^{(i)} + \text{div} \mathbf{j}_{(A)}^{(i)} = 0, \quad (6)$$

where $\mathbf{j}_{(A)}^{(i)}$ is the mass flux vector. We will account for both ordinary and pressure diffusion, and the constitutive equation for the mass flux vectors is given by

$$\mathbf{j}_{(A)}^{(i)} = -D_{(A)} \nabla \rho_{(A)}^{(i)} - M_{(A)} \rho_{(A)}^{(i)} \nabla P^{(i)}. \quad (7)$$

Here, $D_{(A)}$ is the effective diffusion coefficient of species A in the multicomponent mixture, and $M_{(A)}$ the coefficient for pressure diffusion.

Using assumptions (iv) and (vi) we find that the differential energy balance for phase i reduces to

$$T \left(\frac{\partial \bar{P}^{(i)}}{\partial T} \right)_\rho \text{div} \mathbf{v}^{(i)} = \sum_{A=1}^N \psi_{(A)}^{(i)} \text{div} \mathbf{j}_{(A)}^{(i)}, \quad (8)$$

where $\psi_{(A)}^{(i)} = TS_{(A)}^{(i)} + \mu_{(A)}^{(i)}$, $S_{(A)}^{(i)}$ the partial mass entropy of species A , and $\mu_{(A)}^{(i)}$ the chemical potential.

With assumptions (iv) and (v), the differential jump momentum balance for the interface is given by [8,10]

$$2\gamma_0 H \boldsymbol{\xi} - k \boldsymbol{\xi} \text{div}_s \nabla_s H + [[-P \boldsymbol{\xi} + \boldsymbol{\sigma} \cdot \boldsymbol{\xi}] = 0 \quad (9)$$

where div_s is the surface divergence, and ∇_s the surface gradient. The boldface bracket notation is defined as $[[\Psi \boldsymbol{\xi}]] = (\Psi^{(2)} - \Psi^{(1)})\boldsymbol{\xi}$. Combining the x and z component of this balance, and using assumption (iii) we find at $z = h(x, t)$

$$\begin{aligned} \gamma_0 \frac{\partial^2 h(x, t)}{\partial x^2} - \frac{1}{2} k \frac{\partial^4 h(x, t)}{\partial x^4} \\ + \delta P^{(1)} - \delta P^{(2)} + \sigma_{zz}^{(2)} - \sigma_{zz}^{(1)} = 0. \end{aligned} \quad (10)$$

The differential jump mass balance for species A at the interface is given by [assumption (v)] [8]

$$\begin{aligned} (\rho_{(A)}^{(1)} - \rho_{(A)}^{(2)}) \mathbf{v}^s \cdot \boldsymbol{\xi} + (\mathbf{j}_{(A)}^{(2)} - \mathbf{j}_{(A)}^{(1)}) \cdot \boldsymbol{\xi} \\ + (\rho_{(A)}^{(2)} \mathbf{v}^{(2)} - \rho_{(A)}^{(1)} \mathbf{v}^{(1)}) \cdot \boldsymbol{\xi} = 0. \end{aligned} \quad (11)$$

In terms of the parametrization $z = h(x, t)$ we find for the surface velocity $\mathbf{v}^s \cdot \boldsymbol{\xi} = \partial h(x, t)/\partial t$ [assumption (iii)]. For the mass flux vectors in (11), evaluated at the interface, we assume

$$\mathbf{j}_{(A)}^{(i)} \cdot \boldsymbol{\xi} = k_{(A)} (\rho_{(A)}^{(i)} - \bar{\rho}_{(A)}^{(i)}) + \lambda_p \bar{\rho}_{(A)} (\Delta P - \Delta \bar{P}), \quad (12)$$

where λ_p is the permeability of the dividing surface, $\Delta P = P^{(1)} - P^{(2)}$, and $k_{(A)}$ is the mass transfer coefficient for species A . Since the equilibrium dividing surface is a flat interface, we have $\Delta \bar{P} = 0$. Substituting (12) in (11), and linearizing the result, we find

$$\Delta\bar{\rho}_{(A)}\frac{\partial h(x,t)}{\partial t} - k_{(A)}(\delta\rho_{(A)}^{(1)} - \delta\rho_{(A)}^{(2)}) - \lambda_p\Delta\bar{\rho}_{(A)}(\delta P^{(1)} - \delta P^{(2)}) - (\bar{\rho}_{(A)}^{(1)}\nu_z^{(1)} - \bar{\rho}_{(A)}^{(2)}\nu_z^{(2)}) = 0, \quad (13)$$

where $\Delta\bar{\rho}_{(A)} = \bar{\rho}_{(A)}^{(1)} - \bar{\rho}_{(A)}^{(2)}$.

We now introduce the Fourier transformation

$$g(\mathbf{q}, \omega) = \int_{-\infty}^{\infty} e^{i\omega t} dt \int g(\mathbf{r}, t) e^{i\mathbf{q}\cdot\mathbf{r}} d\mathbf{r}. \quad (14)$$

After applying this transformation to (13), the velocity fields can be eliminated using the transform of (5). The transform of (10) is then used to eliminate the pressure difference $(\delta P^{(1)} - \delta P^{(2)})$ in (13). From the resulting expression for $h(q, \omega)$ the power spectrum of the height correlation function can be calculated. The power spectrum is defined as $H(q, \omega) = \langle h(q, \omega)h^*(q, \omega) \rangle$, where $h^*(q, \omega)$ is the complex conjugate of $h(q, \omega)$. We find that (assuming that fluctuations in different phases are not correlated)

$$H(q, \omega) = \sum_A H_{(A)}(q, \omega), \quad (15)$$

$$H_{(A)}(q, \omega) = \frac{1}{\omega^2 + \tau_{(A)}^{-2}} \frac{1}{\Delta\bar{\rho}_{(A)}^2} \times \left[\begin{aligned} &\phi^{(2)2} \Delta\bar{\rho}_{(A)}^2 \langle \delta P^{(1)}(q, \omega) \delta P^{(1)*}(q, \omega) \rangle \\ &+ \phi^{(1)2} \Delta\bar{\rho}_{(A)}^2 \langle \delta P^{(2)}(q, \omega) \delta P^{(2)*}(q, \omega) \rangle \\ &+ \sum_{(i)=(1)}^{(2)} (\theta^2 \langle \sigma_{zz}^{(i)}(q, \omega) \sigma_{zz}^{(i)*}(q, \omega) \rangle + k_{(A)}^2 S_{(AA)}^{(i)}) \\ &+ \bar{\rho}_{(A)}^{(i)2} \mathcal{O}_{zj}^{(i)} \langle f_j^{h(i)}(q, \omega) f_j^{h(i)*}(q, \omega) \rangle \mathcal{O}_{jz}^{(i)} \end{aligned} \right]. \quad (16)$$

Here $\tau_{(A)}$ is a relaxation time given by

$$\tau_{(A)}^{-1} = [\lambda_p + \phi^{(1)} + \phi^{(2)}] q_x^2 \left(\gamma_0 + \frac{1}{2} k q_x^2 \right) \quad (17)$$

and $\phi^{(i)} = \bar{\rho}_{(A)}^{(i)} \Delta\bar{\rho}_{(A)}^{-1} (\nu^{(i)} + 2\eta^{(i)})^{-1} q_z^{-1}$. Equation (17) is a generalization of the expression derived in [11] for the relaxation time of a membrane, and the semiempirical expression in [4]. The correlation function $S_{(AA)}^{(i)}(q, \omega)$ is defined as $\langle \delta\rho_{(A)}^{(i)}(q, \omega) \delta\rho_{(A)}^{(i)*}(q, \omega) \rangle$, and the function θ equals $\Delta\bar{\rho}_{(A)}(\lambda_p + \phi^{(1)} + \phi^{(2)})$. In the last term of (16) we sum over the index $j = x, z$. The tensor $\mathcal{O}_{ij}^{(i)}$ is given by

$$\mathcal{O}_{ij}^{(i)} = \frac{1}{\eta^{(i)} q^2} \left(\delta_{ij} - \frac{\nu^{(i)} + \eta^{(i)}}{\nu^{(i)} + 2\eta^{(i)}} \frac{q_i q_j}{q^2} \right). \quad (18)$$

The sum in (15) is over all components being transferred across the interface. On short time scales water is usually the only component being transferred [4]. On longer time scales the transfer of the biopolymers is also affecting the behavior of the system [6].

TABLE I. Experimental data for the gelatin-dextran-water system [4].

	Sample 2		Sample 6	
	Phase 1	Phase 2	Phase 1	Phase 2
$\rho_{(w)}^{(i)}$ (Kg/m ³)	952.3	944.2	925.1	909.9
$\rho_{(\text{gel})}^{(i)}$ (Kg/m ³)	22.0	50.0	11.7	105.3
$\rho_{(\text{dex})}^{(i)}$ (Kg/m ³)	37.5	16.0	93.8	3.1
$\eta^{(i)}$ (10 ⁻³ Pas)	7.45	8.18	34.80	25.95
$\nu^{(i)}$ (10 ⁻³ Pas)	17.38	19.08	81.20	60.56
λ_p [10 ⁻³ m ³ /(Ns)]		3.4		0.1
γ_0 (10 ⁻⁶ N/m)		0.2		9.2
k (k _B T)		200		200

From the fluctuation-dissipation theorem (see, for example, [12]), and the Fourier transform of (5), (6), and (8), we find

$$H_{(A)}(q, \omega) = \frac{k_B T}{\omega^2 + \tau_{(A)}^{-2}} \frac{1}{\Delta\bar{\rho}_{(A)}^2} \left[\begin{aligned} &\frac{\phi^{(1)2} \epsilon^{(2)} \Delta\bar{\rho}_{(A)}^2}{\bar{\rho}^{(2)}} \\ &+ \frac{\phi^{(2)2} \epsilon^{(1)} \Delta\bar{\rho}_{(A)}^2}{\bar{\rho}^{(1)}} + \sum_{(i)=(1)}^{(2)} \left(2\theta^2 (\nu^{(i)} + 2\eta^{(i)}) \right. \\ &+ \frac{k_{(A)}^2 \alpha_{(A)}^{(i)}}{\bar{\rho}^{(i)}} (1 + M_{(A)}^2 q^2 \epsilon^{(i)}) \\ &\left. + \bar{\rho}_{(A)}^{(i)2} \mathcal{O}_{zj}^{(i)} \left[\frac{q_j^2 \epsilon^{(i)}}{\bar{\rho}^{(i)}} - 2q^2 (\nu^{(i)} + 2\eta^{(i)}) \right] \mathcal{O}_{jz}^{(i)} \right) \end{aligned} \right], \quad (19)$$

where k_B is the Boltzmann constant, $\alpha_{(A)}^{(i)} = \bar{\rho}_{(A)}^{(i)2} q^2 / (\omega^2 + q^4 D_{(A)}^2)$, and

$$\epsilon^{(i)} = \frac{T^2 (\frac{\partial P}{\partial T})_{\rho}^2 - \sum_{A=1}^N \psi_{(A)}^{(i)2} q^2 D_{(A)}^2 \alpha_{(A)}^{(i)}}{\sum_{A=1}^N \psi_{(A)}^{(i)2} q^2 M_{(A)}^2 (q^2 D_{(A)}^2 \alpha_{(A)}^{(i)} + \bar{\rho}_{(A)}^{(i)2})}. \quad (20)$$

In arriving at this result we have assumed that the correlations between different components are zero. To illustrate

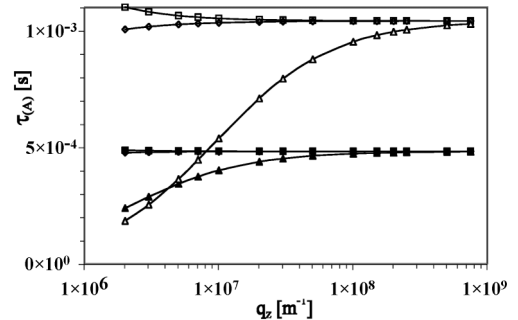


FIG. 1. Relaxation time $\tau_{(A)}$ as a function of q_z for dextran (\diamond), gelatin (\square), and water (\triangle), at a fixed value of $q_x = 10^6 \text{ m}^{-1}$. Filled symbols: sample 2; open symbols: sample 6.

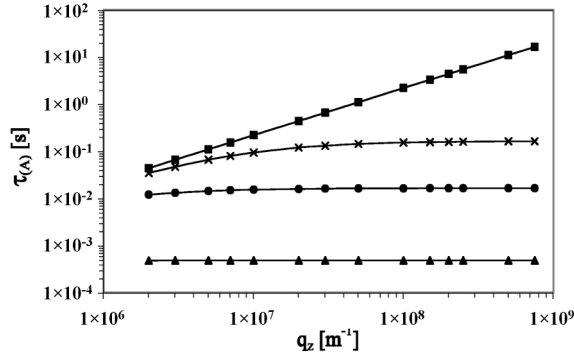


FIG. 2. Relaxation time $\tau_{(A)}$ as a function of q_z for dextran (sample 2), at a fixed value of $q_x = 10^6 \text{ m}^{-1}$. From top to bottom: $\lambda_p = 0$, $\lambda_p = 10^{-5}$, $\lambda_p = 10^{-4}$, $\lambda_p = 3.4 \times 10^{-3} \text{ m}^3/(\text{Ns})$.

the effect of permeability, surface tension, and bending rigidity on the fluctuations, we will calculate the relaxation time $\tau_{(A)}$ for a phase-separated gelatin-dextran-water system [4]. The data used for the calculation are the data for sample 2 and 6 in [4], and are given in Table I. Sample 2 is a mixture with composition (prior to separation) close to the critical point of the system, and sample 6 is a sample far away from the critical point. The values for the shear viscosities $\eta^{(i)}$ were calculated from the relative viscosities reported in [4], using a value for the shear viscosity of water equal to $0.89 \text{ mPa} \cdot \text{s}$ ($T = 25^\circ \text{C}$). Experimental data for the bulk viscosities of the upper and lower phases are not available, so we use a common approximation that for aqueous systems $\eta_b^{(i)} \approx 3\eta^{(i)}$. Data for the bending rigidity are also not available, so we used a rough estimate of this parameter based on experimental results presented in [2]. In Fig. 1 the relaxation time $\tau_{(A)}$ is plotted as a function of q_z , at a fixed value for $q_x = 10^6 \text{ m}^{-1}$, for all components in sample 2 and 6. We see that at high q values the relaxation is completely dominated by the permeability term. For water the viscosity terms $\phi^{(i)}$ are relatively more important than for the polymers because the densities for water in the mixture are much higher. In Fig. 2 the relaxa-

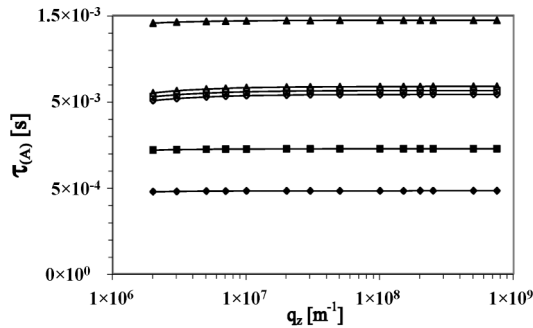


FIG. 3. Relaxation time $\tau_{(A)}$ as a function of q_z for dextran, at a fixed value of $q_x = 10^6 \text{ m}^{-1}$. Filled symbols: sample 2; open symbols: sample 6. Values of k : 0 (Δ), $100k_B T$ (\square), and $200k_B T$ (\diamond).

tion time of dextran (sample 2) is plotted for various values of the permeability. The bottom curve is the plot for $\lambda_p = 3.4 \times 10^{-3} \text{ m}^3/(\text{Ns})$, the value determined in [4]. We see that when we set λ_p to zero in (17), the relaxation time increases by several orders of magnitude. Finally, in Fig. 3 we have plotted the relaxation time for dextran, for both systems, and values of the bending rigidity of 0 , 100 , and $200k_B T$. We see that $\tau_{(A)}$ in system 2 (close to the critical point) is very sensitive to variations in k . The relaxation in this system is dominated by the permeability and bending rigidity, and we find that $\tau_{(A)}$ scales as $\tau_{(A)}^{-1} \sim \lambda_p k q_x^4$. With $q_x = 1/L_x$, where L_x is the wavelength of the perturbations, we find $\tau_{(A)} \sim L_x^4/(\lambda_p k)$, a scaling that is in agreement with the scaling found for rigidity and permeability dominated coarsening during phase separation in [5]. Sample 6 is almost insensitive to the value of the bending rigidity. In this system relaxation is clearly dominated by permeability and surface tension, and we find $\tau_{(A)} \sim L_x^2/(\lambda_p \gamma_0)$, also in agreement with [5].

This analysis shows conclusively that mass transfer has an important effect on the dynamic behavior of water-in-water emulsions, like phase-separated (bio)polymer solutions, liposomes, polymersomes, or colloidosomes. In the expression for the relaxation time $\tau_{(A)}$, contributions from the elasticity of the interface were neglected [see assumption (v)]. These terms could be important for polymersomes or colloidosomes, especially in the low q and high ω regime. These contributions can be accounted for by incorporating an appropriate expression for the surface stress tensor in the jump momentum balance (9), like, for example, a linear viscoelastic model, that incorporates the elastic effects through the surface dilatational modulus and surface shear modulus [8].

-
- [1] E. Scholten, J.E. Visser, L.M.C. Sagis, and E. van der Linden, *Langmuir* **18**, 2234 (2002).
 - [2] E. Scholten, L.M.C. Sagis, and E. van der Linden, *J. Phys. Chem. B* **108**, 12 164 (2004).
 - [3] E. Scholten, L.M.C. Sagis, and E. van der Linden, *Macromolecules* **38**, 3515 (2005).
 - [4] E. Scholten, J. Sprakel, L.M.C. Sagis, and E. van der Linden, *Biomacromolecules* **7**, 339 (2006).
 - [5] E. Scholten, L.M.C. Sagis, and E. van der Linden, *J. Phys. Chem. B* **110**, 3250 (2006).
 - [6] E. Scholten, L.M.C. Sagis, and E. van der Linden, *Biomacromolecules* **7**, 2224 (2006).
 - [7] E.G. Flekkøy and D.H. Rothman, *Phys. Rev. Lett.* **75**, 260 (1995); see also *Phys. Rev. E* **53**, 1622 (1996).
 - [8] J.C. Slattery, *Interfacial Transport Phenomena* (Springer, New York, 1990).
 - [9] W. Helfrich, *Langmuir* **20**, 2292 (2004).
 - [10] L.M.C. Sagis, *Physica (Amsterdam)* **246A**, 591 (1997).
 - [11] J. Prost, J.-B. Manneville, and R. Bruinsma, *Eur. Phys. J. B* **1**, 465 (1998).
 - [12] B.J.A. Zielinska and D. Bedeaux, *Physica (Amsterdam)* **112A**, 265 (1982).